Planta (2022) 256: 53
https://doi.org/10.1007/s00425-022-03962-8

ORIGINAL ARTICLE

Single-base methylome analysis reveals dynamic changes of genome-wide DNA methylation associated with rapid stem growth of woody bamboos

Liang-Zhong Niu[1,2] · Wei Xu[1] · Peng-Fei Ma[1] · Zhen-Hua Guo[1,2] · De-Zhu Li[1,2]

Received: 17 January 2022 / Accepted: 14 July 2022 / Published online: 1 August 2022
© The Author(s), under exclusive licence to Springer-Verlag GmbH Germany, part of Springer Nature 2022

Abstract

Main conclusion **CG and CHG methylation levels in the rapid shoot growth stages (ST2–ST4) of woody bamboos were obviously decreased, which might regulate the internode elongation during rapid shoot growth, while CHH methylation was strongly associated with shoot developmental time or age.**

Abstract DNA methylation plays a critical role in the regulation of plant growth and development. Woody bamboos have a unique trait of rapid stem growth resulted from internode elongation at the shooting period. However, it is still unclear whether DNA methylation significantly controls the bamboo rapid stem growth. Here we present whole-genome DNA methylation profiles of the paleotropical woody bamboo *Bonia amplexicaulis* at five newly defined stages of shoot growth, named ST1–ST5. We found that CG and CHG methylation levels in the rapid shoot growth stages (ST2–ST4) were significantly lower than in the incubation (ST1) and plateau stages (ST5). The changes in methylation levels mainly occurred in flanking regions of genes and gene body regions, and 23647 differentially methylated regions (DMRs) were identified between ST1 and rapid shoot growth stages (ST2–ST4). Combined with transcriptome analysis, we found that DMR-related genes enriched in the auxin and jasmonic acid (JA) signal transduction, and other pathways closely related to plant growth. Intriguingly, CHH methylation was not involved in the rapid shoot growth, but strongly associated with shoot developmental time by gradually accumulating in transposable elements (TEs) regions. Overall, our results reveal the importance of DNA methylation in regulating the bamboo rapid shoot growth and suggest a role of DNA methylation associated with development time or age in woody bamboos.

Keywords DNA methylation · Gene expression · Internode elongation · Jasmonic acid · Woody bamboos

Abbreviations

BS	Bisulfite
DEG	Differentially expressed gene
DML	Demeter-like
DMRs	Differentially methylated regions
JA	Jasmonic acid
JAZ	Jasmonate ZIM-domain
RdDM	RNA-directed DNA methylation pathway
ST1	Incubation stage
ST2	Early stage of rapid shoot growth
ST3	Middle stage of rapid shoot growth
ST4	Late stage of rapid shoot growth
ST5	Plateau stage of shoot growth
TE	Transposable element

Communicated by Dorothea Bartels.

✉ Zhen-Hua Guo
guozhenhua@mail.kib.ac.cn

✉ De-Zhu Li
DZL@mail.kib.ac.cn

[1] Germplasm Bank of Wild Species, Kunming Institute of Botany, Chinese Academy of Sciences, 132 Lanhei Road, Kunming 650201, Yunnan, China

[2] University of Chinese Academy of Sciences, Beijing 100049, China

Introduction

5´ Cytosine methylation is a conservative feature of eukaryotic genomes and plays a crucial role in the inhibition of transposable elements (TEs), regulation of gene expression, especially genomic imprinting, and response to

environmental stress including biotic or abiotic stress during plant growth and development (Cedar and Bergman 2012). 5´ Cytosine methylation usually occurs in the symmetric CG context in both plants and animals. However, considerable methylcytosines are also found in the contexts of CHG and CHH nucleotide loci in plants, where H means A, T or C (Feng et al. 2010; Law and Jacobsen 2010). In plants, cytosine is de novo methylated through the RNA-directed DNA methylation pathway (RdDM) and is maintained by different DNA methylation-related enzymes (Zhang et al. 2018). Studies in *Arabidopsis* and other model plant species have revealed that CG methylation was maintained through methyltransferase1 (MET1) (Finnegan and Dennis 1993; Kankel et al. 2003) and that CHG methylation was maintained through chromomethylase3 (CMT3), a plant-specific enzyme that depends on histone H3K9 di-methylation (H3K9me2) (Lindroth et al. 2001; Jackson et al. 2004; Ebbs et al. 2005; Du et al. 2012; Stroud et al. 2013, 2014). CHH methylation is established by the RdDM pathway to guide domains rearranged by methyltransferase1 (DRM1) and DRM2 to perform their functions. In addition, evidence has shown that CHH methylation can also be established in an independent RdDM pathway by CMT2 (Cao and Jacobsen 2002; Xie et al. 2004; Zemach et al. 2013; Matzke and Mosher 2014). On the other hand, cytosine methylation could be removed by a type of DNA glycosylase/demethylase, including Repressor of Silencing 1 (ROS1), Demeter-like 2 (DML2), DML3 and Demeter (DME) (Choi et al. 2002; Gong et al. 2002; Penterman et al. 2007; Ortega-Galisteo et al. 2008). Therefore, the activities of DNA methyltransferases and glycosylases are closely linked to the extent and pattern of genomic DNA methylation.

Many studies have found that DNA methylation plays a central role in regulating plant growth and development. For example, the disruption of *Met1* gene expression in *Arabidopsis* caused abnormal vegetative and reproductive growth (Finnegan et al. 1996), similar as in other model plants, such as tobacco (Nakano et al. 2000) and rice (Yamauchi et al. 2014). In rice, the knockdown of *OsDCL3a* displayed pleiotropic phenotypes affecting crucial agricultural traits, including larger flag leaf angle, fewer secondary branches and dwarf phenotypes (Wei et al. 2014). As the gene encoding DRM2 was silenced in rice, the plants exhibited a reduced number of tillers, delayed heading, abnormal panicle and spikelet, and complete sterility (Moritoh et al. 2012). In addition, the DNA methylation pathway active during reproduction plays a vital role during the development of gametophytes in maize (Garcia-Aguilar et al. 2010). Plants containing mutants in DNA methylation pathway genes (e.g., *Zmet2* and *Zmet5*) exhibited a loss of a large number of methylation sites, and the severe methylome changes in maize may have a stronger harmful phenotypic effect than in *Arabidopsis* (Li et al. 2014).

Regarding DNA demethylases, studies have shown that Demeter (DME) is specifically expressed in the central cells of developing female gametophytes and is essential for seed development and the expression of imprinted genes; its mutation could result in the abortion and abnormal development of seeds (Park et al. 2016). Furthermore, DNA methylation can also participate in the regulation of plant growth and development by activating or suppressing the expression of specific genes. For example, ripening-associated DNA hyper-methylation plays crucial roles in sweet orange fruit ripening by repressing the expression of photosynthesis genes (Huang et al. 2019). However, DNA demethylation mediated by *SlDML2* is crucial during tomato fruit ripening, and it is essential for both the suppression of ripening-repressed genes and the activation of ripening-induced genes (Lang et al. 2017).

Here, we focus on the woody bamboos. Bamboos are the general term for plants in the subfamily Bambusoideae within the grass family Poaceae, which have important cultural, ecological and economic value (Li et al. 2006). To date, more than 1690 species of bamboos have been identified worldwide and are classified into one herbaceous lineage and three woody lineages (Guo et al. 2019; Soreng et al. 2022). Compared with other grasses, woody bamboos have many unique traits, including rapid stem (culm) growth at the shooting period, high culm lignification at maturity, and long phase of vegetative growth with a flowering cycle of 30–60 years and even up to 120 years in some species (Janzen 1976). In particular, the underground rhizome bearing young stems (shoots) in woody bamboos has a strong meristematic reproductive ability (Janzen 1976). Researchers have long been fascinated by the rapid stem growth of woody bamboos, which can grow up to 1 m in height within 24 h, as a result of internode elongation of young shoots (Peng et al. 2013a; Jin et al. 2021). Previous studies have mainly concentrated on the clarification of shoot growth patterns and the microscopic observation of woody stems (Murphy and Alvin 1992; Lin et al. 2002; Cui et al. 2012). Recently, molecular studies identified several candidate genes related to shoot growth, such as *BoSus*, *BoPAL1*, *BoPAL2* and *BoSUT2* (Chiu et al. 2006; Gao et al. 2010; Hsieh et al. 2010a, b, 2011). It was also found that many metabolic pathways of cell wall biosynthesis were related to the rapid shoot growth of woody bamboos (Cui et al. 2012). In addition, genes encoding key enzymes for lignin and cellulose biosynthesis and plant hormones were suggested to play a central role in the rapid shoot growth of woody bamboos (Liu et al. 2012; Peng et al. 2013b). Furthermore, a recent study identified 1622 bamboo-specific orphan genes and revealed that the interaction between these new genes and the whole genome duplicates (WGDs) of woody bamboos played a key role in rapid stem growth (Jin et al. 2021). In another recent study,

a focus was given to the unique trait of a long phase of vegetative growth of moso bamboo, *Phyllostachys edulis* (Zhang et al. 2021). However, whether DNA methylation is involved in the regulation of shoot elongation in woody bamboos remains largely unclear. Therefore, our main aim was to investigate the DNA methylation profiles associated with bamboo rapid stem growth.

In this study, we used *B. amplexicaulis*, a clump-forming paleotropical woody bamboo as the target species, primarily due to its genome has been recently sequenced (Guo et al. 2019). Integrating the genome-wide cytosine methylation with transcriptome analyses revealed that DNA methylation was closely associated with rapid shoot growth and that CHH methylation gradually accumulates in most TE regions during rapid shoot growth in a time/development-dependent manner.

Materials and methods

Plant materials

Young stems (shoots) of *B. amplexicaulis* (L. C. Chia et al.) N. H. Xia at different growth stages were obtained from the field of Xiaoliancheng, Longzhou County, Guangxi Zhuang Autonomous Region, China. The growth curve of internodes in the stem growth stages of *B. amplexicaulis* was obtained through observing its growth status throughout the growth season (Fig. 1). Stems at five different developmental stages, i.e., the growth incubation period, the early, middle, late stages and the plateau period of rapid stem growth (Fig. S1), were collected and immediately frozen in liquid nitrogen and then stored at − 80 °C for subsequent RNA and DNA extraction. Samples for each stage were collected from different

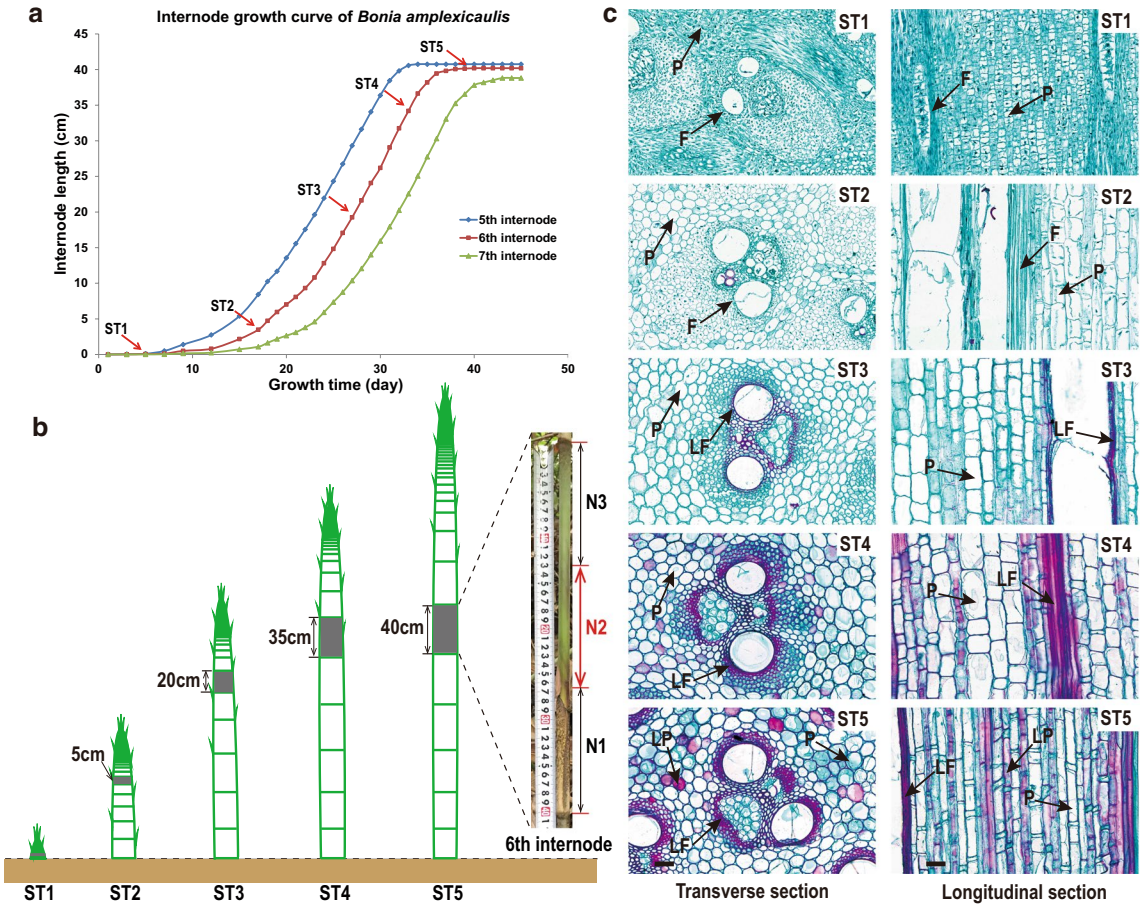

Fig. 1 Anatomical observation of shoot growth of *B. amplexicaulis* and sampling strategy. **a** Internode growth curve of *B. amplexicaulis*. The blue, red and green lines represent the 5th, 6th, and 7th internode of the young stem (culm), respectively. We chose the 6th internode as the experimental material, and the sampling time of five representing developmental stage (ST1–ST5) is indicated above the growth curve. **b** Sampling strategy of the 6th internode for subsequent analyses. The height of each stage of the 6th internode is indicated. At each developmental stage, the 6th internode is divided into three parts, N1, N2 and N3 with equal length from base to top and part N2 was used as the experimental material. **c** Transverse and longitudinal sections of tissue from ST1 to ST5. *F* fiber cells, *LF* lignification of fiber cells, *P* parenchyma cells, *LP* lignification of parenchyma cells. Scale bars: 50 μm

bamboo shoots, and five shoots were collected as replicates from the same bamboo clump.

Sectioning and microscopic observation

Approximately 1 cubic centimeter of *B. amplexicaulis* stem tissue samples were prepared and fixed in FAA fixation solution (70% ethanol, glacial acetic acid and formaldehyde, 18:1:1, by vol.). The fixed tissues were dehydrated using ethanol with gradually increasing concentrations. Then tissues were embedded in paraffin by an encapsulation machine (JB-P5, Wuhan Junjie Electronics Co., Ltd.). Longitudinal and transverse sections of 10 μm in thickness were obtained by a pathological slicer (RM2016, Shanghai Leica Instruments Co., Ltd.). The sections were deparaffinized and stained with a safranin O staining solution for 15–30 s and a plant solid green staining solution for 6–20 s, respectively. Finally, the sections were sealed with neutral balsam and watched by CaseViewer software after using the Imaging systems (DS-U3, Nikon, Tokyo, Japan) scanning.

DNA extraction and bisulfite (BS) sequencing

We extracted total shoot DNA from liquid nitrogen quick-frozen internodes using the Plant Genomic DNA Kit (DP305-02, Tiangen, Beijing, China) according to the instruction manual. The concentration and purity of DNA were measured by Qubit® DNA Assay Kit (Life Technologies, Carlsbad, CA, USA) and NanoPhotometer® spectrophotometer (Implen, Westlake Village, CA, USA). Qualified 100 ng DNA mixed with 0.5 ng lambda DNA was fragmented into 200–300 bp fragments by sonication through a Covaris S220 sonicator. Then, an EZ DNA Methylation-GoldTM Kit (Zymo Research, Irvine, CA, USA) was used to treat these DNA fragments with BS. For each sample, we designed two biological replicates and correspondingly constructed two BS-seq libraries. Finally, constructed sequencing libraries were performed at the Illumina Novaseq platform with paired-ended 150 bp sequences at Novogene Technology Co., Ltd. (Beijing, China).

BS-seq mapping and analysis

FastQC (fastqc_v0.11.5) was used to filter raw data reads to obtain clean reads. Then, Bismark software (version 0.21.0) (Krueger and Andrews 2011) with default parameters was used to align bisulfite-treated clean reads to the *B. amplexicaulis* genome (Guo et al. 2019). The reference the *B. amplexicaulis* genome was converted into a BS-treated version (C converted T and G converted A) and then Bowtie2 (Langmead and Salzberg 2012) was used to build the index. Correspondingly, a BS-treated version was obtained from the sequence reads and these reads were aligned to the reference genome with a manner of directional. Finally, the cytosine methylation information of each site was extracted. DMRs were identified by the methylKit package (Akalin et al. 2012) in R software (https://www.r-project.org), which detects DMRs with a dynamic fragment strategy of 500 bp as the window and 500 bp as the step size. T test was applied to filter significant DMRs by q value = 0.01 and methylation difference threshold percentage (methdiff) = 25 as the standard for CG and CHG contexts, while difference = 10 for CHH context. After that, the genes associated with DMRs were identified using BEDTools (Quinlan and Hall 2010). Then we used OmicShare (http://www.omicshare.com/tools) to perform KEGG enrichment analysis of these DMR-associated genes. The methylation levels in different genomic regions including gene and TE regions were obtained using ViewBS software (Huang et al. 2018) and graphics were generated using the ggplot2 package (Ginestet 2011) in R software. IGV software (Thorvaldsdottir et al. 2013) was used to display the DNA methylation levels in gene and TE regions and flanking regions. We used ViewBS software to obtain the methylation levels for all TEs, and screened TEs with a gradual increase in CHH methylation levels based on the criteria where a given TE has the highest methylation level in ST5, followed by ST4, ST3, ST2, with the lowest in ST1.

RNA extraction and RNA-seq analysis

Transcriptome sequencing with three biological replicates for each stage was performed with the same materials as DNA methylation sequencing. Using an E.Z.N.A.® Plant RNA Kit (R6827-01, Omega Biotech, Norcross, GA, USA), total RNA was extracted according to the instruction manual. The integrity and purity of RNA were measured by an RNA Nano 6000 Assay Kit (Agilent Technologies, Santa Clara, CA, USA) and a NanoPhotometer® spectrophotometer (Implen). Total 1 μg qualified RNA sample was prepared for each sample to construct the transcriptome library and then sequencing was conducted by Novogene Technology Co., Ltd. In short, magnetic beads and high temperature were used for RNA purification and fragmentation. The double-stranded cDNA of each target fragment (250–300 bp) was synthesized and purified. Sequence libraries were constructed using the NEBNext® UltraTM RNA Library Prep Kit for Illumina® (NEB, Ipswich, MA, USA) according to the instruction manual. Then constructed libraries were sequenced on the Illumina NovaSeq platform and reads with 150 bp paired-end were generated. Trimmomatic (Bolger et al. 2014) was used to filter raw reads and then to generate clean reads. These clean reads were mapped to the *B. amplexicaulis* genome (http://www.genobank.org/bamboo) using HISAT2 (version 2.2.1) (Kim et al. 2019). Differentially expressed genes (DEGs) were identified by DEseq2

(Varet et al. 2016), with screened criteria as fold change ≥ 2 and padjs < 0.01.

Analysis of the relationship between DNA methylation and gene expression

All genes in the *B. amplexicaulis* genome *were* divided into non-expressed genes (transcripts per million (TPM) < 0.1) and expressed genes with five groups according to their transcription levels. The first group represents the group with the lowest transcription levels, while the 5th group represents the group with the highest transcription levels. The transcription levels were as follows: 1st group (0.1 < TPM < 25), 2nd group (25 < TPM < 50), 3rd group (50 < TPM < 100), 4th group (100 < TPM < 500) and 5th group (500 < TPM).

Identification of DNA methylation-related genes in the *B. amplexicaulis* genome

First, we obtained the protein sequences of the DNA methylation-related genes in the rice genome (http://riceplantbiology.msu.edu), then used the Blastp program to search the protein database of *B. amplexicaulis* (*B. amplexicaulis* genomic data online website: http://www.genobank.org/bamboo) (Guo et al. 2019). All the candidate proteins were predicted using the online branching software SMART (http://smart.embl-heidelberg.de/) (Letunic et al. 2004) and Pfam (http://pfam.xfam.org) (Mistry et al. 2021) for their conserved protein domains. In addition, the online website (http://meme-suite.org/) MEME (Bailey et al. 2006) was applied to predict its motif, and we used MEGA 6.0 (Tamura et al. 2013) software to perform sequence alignment to construct a neighbor-joining phylogenetic tree with 1000 bootstrap replicates.

Quantitative real-time PCR analysis

The GoScript™ Reverse Transcription Kit (Promega Biotechnology, Beijing, China) was used for reverse transcription of DNase digested RNA. Primer design was carried out using Primer6 software and the primer sequences were synthesized through Beijing Tsingke Biotechnology Co., Ltd. The specific primer sequences information was shown in Table S1. The GoTaq® qPCR Master Mix Kit from Promega Biotechnology was used for real-time quantitative PCR (qRT-PCR) reactions. Three biological replicates and two technical replicates were performed for each sample. The specific PCR reaction procedure was as follows: predenaturation at 95 °C for 10 min, then denaturation at 95 °C for 15 s, and annealing at 60 °C for 1 min for a total of 40 cycles. In our study, the UBC (*Bam040291*) gene of *B. amplexicaulis* was used as an internal reference gene.

Results

The growth pattern of *B. amplexicaulis* internodes

To investigate the role of the DNA methylation in the rapid shoot growth of *B. amplexicaulis*, we first investigated the growth rate of internodes from the incubation stage to the final growth stage. The whole stem growth of *B. amplexicaulis* is the result of elongation of its internodes, where base internodes elongate first and then the top ones. Therefore, the growth period of a specific internode can represent the whole stem growth period of *B. amplexicaulis*. We selected the representative 5th, 6th and 7th internodes approximately at the breast-height of its stem to record their length daily (Fig. 1a). The growth of *B. amplexicaulis* stem is completed within about two months and a slow–fast–slow curve (sigmoid growth curve) of growth was observed, in consensus with the observation in other woody bamboos (Li and Guo 2014; Tang et al. 2015). We found that there is a similar growth curve of 5th, 6th and 7th internode and thus selected the 6th internode at the breast height for subsequent analyses. Upon the growth curve of the 6th internode, here we defined five stages, named as ST1-ST5 (Fig. 1b) for precise characterization of rapid shoot growth of woody bamboos. The ST1 represents the growth incubation stage of the internode with a slow growth rate. From ST2 to ST4, the internode undergoes rapid growth, corresponding to early, middle and late stages of rapid growth with ~ 5 cm, ~ 20 cm and ~ 35 cm of internode length, respectively. From ST4 to ST5, the growth rate of the internode sharply decelerated and finally reached ~ 40 cm at ST5. From ST1 to ST5, the parenchyma cells gradually elongated and were accompanied by an increase in the degree of culm lignification (Fig. 1c), consistent with observation in other woody bamboos (Cui et al. 2012).

Features of the *B. amplexicaulis* shoot DNA methylome

With the growth patterns observed, we performed genome-wide DNA methylation sequencing for five development stages of the 6th internode. To ensure more accurate sampling, the internode was divided into three parts with equal length and named as N1, N2, N3 from base to top. All samples collected from the N2 part with two biological replicates (Figs. 1b; S1). After BS DNA methylation sequencing, we obtained ~ 200 million clean reads for each sample, yielding ~ 27–35 Gb of data. There was a strong correlation between two biological replicates (Fig. S2), suggesting our data were credible for subsequent analyses.

Upon the clean reads mapping, we observed a > 30 × coverage of *B. amplexicaulis* genome (with an estimated genome size of 850.4 Mb; Table S2), which covered > 82% of the genome.

The global methylation analysis showed bulk methylation in the *B. amplexicaulis* genome with ~ 69% CG, 44% CHG and 3% CHH, respectively (Fig. 2a, b; Table S3). As shown in Fig. 2a, the landscapes of CG, CHG and CHH methylation exhibited nearly identical distribution in *B. amplexicaulis* genome across five stages of stem growth in terms of internode development. These methylated cytosines mainly occurred in the context of CG and CHG sites, accounted for 53% and 37% of total methylated cytosines, while only a small fraction of total methylated cytocines (10%) was at CHH contexts. During the rapid shoot growth (ST2–ST4), the overall reduction of CG and CHG methylation was relative to the incubation stage (ST1) and plateau stage (ST5) (Fig. 2b). Interestingly, we discovered that the proportion and methylation levels of CHH gradually increased from ST1 to ST5 (Fig. 2b, c).

To further investigate DNA methylation patterns in trinucleotide contexts, we divided the CG, CHG and CHH methylation of *B. amplexicaulis* into different sub-contexts as shown in Fig. S3. We found that the CGA motif had the highest densities among the CG sub-contexts, though all CG sub-contexts had comparable methylation levels across the genome (Fig. S3). For the CHG contexts, the density and methylation level of CCG motifs were much lower than those of CAG and CTG throughout the scaffolds, consistent with the result reported in *Arabidopsis* and other plants (Gouil and Baulcombe 2016). For the CHH contexts, CAA and CCC had the highest and lowest densities throughout the whole genome, respectively, and cytosines in CCH were less methylated compared to CTH and CAH. These results clearly showed the methylation of the middle C would affect the methylation of adjacent C though underlying molecular mechanism remained unknown.

DNA methylation profiles in gene and TE regions

We inspected the distribution of CG, CHG, and CHH methylations in gene and TE regions and their flanking regions within 2 kb. Two biological replicates exhibited nearly identical profiles of DNA methylation (Figs. 3; S4). As shown in Fig. 3, CG methylation occurred preferentially in the gene body regions relative to the flanking regions, while CHG and CHH methylation exhibited the higher levels in flanking regions than in gene body regions. DNA methylation

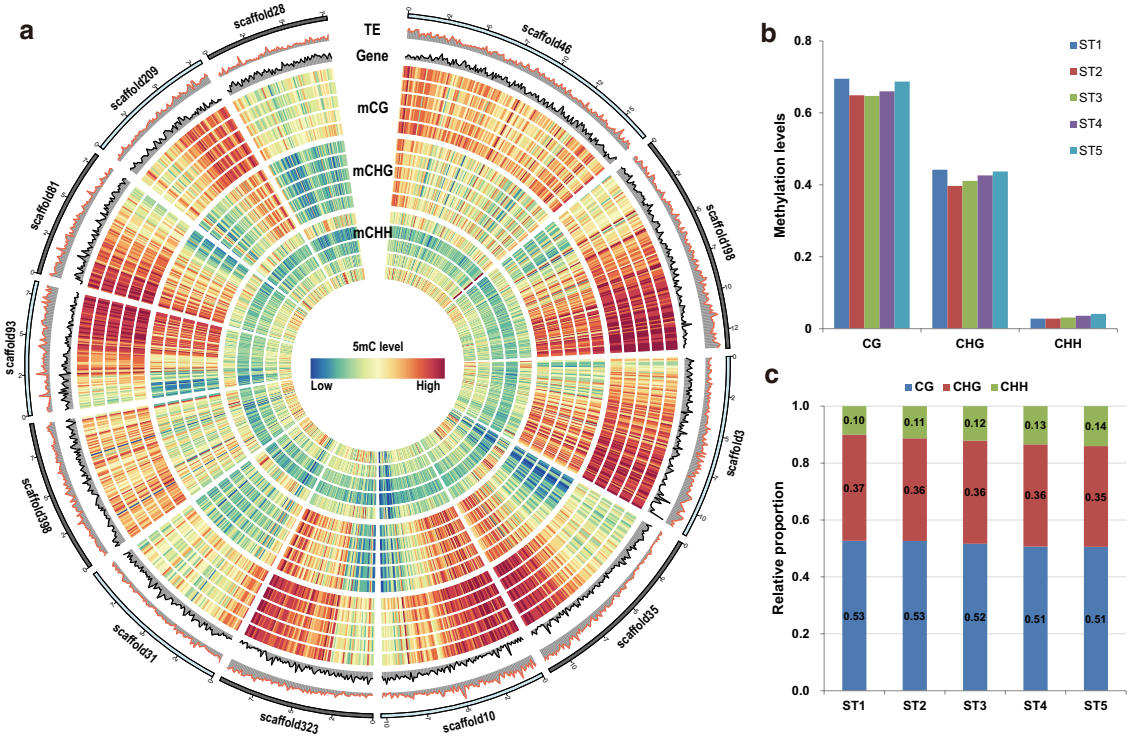

Fig. 2 DNA methylation landscape of the *B. amplexicaulis* genome. **a** DNA methylation profiles of the CG, CHG and CHH DNA across the top 12 scaffolds of *B. amplexicaulis*. Methylation levels of CG, CHG and CHH contexts at different developmental stages (ST1–ST5) are indicated from outer to inner rings. The density within a-100 kb window of transposable elements (TEs) and genes are also displayed. **b** Average methylation levels of CG, CHG and CHH contexts of five developmental stages (ST1–ST5). **c** Relative proportion of CG, CHG and CHH contexts of five developmental stages (ST1–ST5)

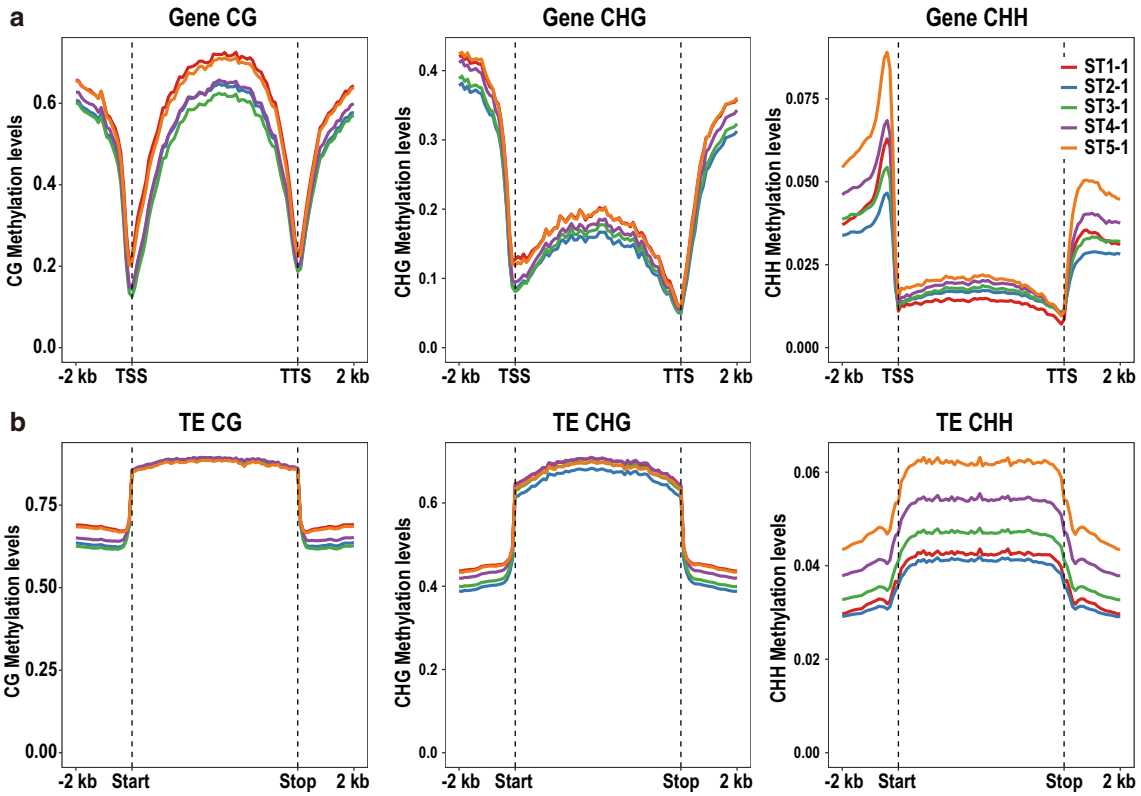

Fig. 3 DNA methylation profiles in genes and TEs. **a** DNA methylation patterns across genes and their flanking regions within 2 kb. **b** DNA methylation patterns across TEs and their flanking regions within 2 kb. The average methylation levels for each 100-bp interval are plotted. The dashed line indicates the transcription start site (TSS) or transcription termination site (TTS)

levels were the lowest near transcriptional start site (TSS) and transcriptional terminal site (TTS). Nevertheless, DNA methylation extents of the CG, CHG, and CHH contexts were markedly higher in TE regions relative to their flanking regions, especially CG and CHG contexts which were heavily methylated in TE regions.

During rapid elongation of the internode, we observed that CG and CHG methylation in incubation stage (ST1) and plateau stage (ST5) had significantly higher levels than in the rapid shoot growth stages (ST2–ST4) in both gene body and flanking regions (Fig. 3), while CHH methylation levels were gradually elevated in gene body and flanking regions during the internode development (Fig. 3). In contrast to gene body regions, the TEs were stably and highly methylated in CG and CHG sequence context across the whole developmental stages, but CG and CHG methylation in their flanking regions have an obvious decrease in ST2–ST4 relative to ST1 and ST5 (Fig. 3). Notably, CHH methylation level in the TE and flanking regions exhibited a gradual increasing trend.

In sum, we found an obvious decrease of CG and CHG methylation levels in gene body and flanking regions during bamboo rapid shoot growth (ST2–ST4), suggesting that DNA methylation may be associated with the rapid shoot growth of woody bamboos. Interestingly, CHH methylation gradually accumulating in TE regions may be associated with the developmental stage or age in woody bamboos.

Methylation profiles in different TEs during internode development in *B. amplexicaulis*

To gain insights into understanding the relationship between DNA methylation and TEs, especially the relationship between CHH methylation in TEs and development time or age, we profiled the DNA methylation pattern in different classes of TEs in the *B. amplexicaulis* genome (Fig. 4a). In the genome, class I type TEs were dominant and LARD, LTR_Copia and LTR_Gypsy were abundant (352,742 for LARD, 351,966 for LTR_Copia and 203,941 for LTR_Gypsy). We subsequently detected the average methylation level of each TE type and found a relatively stable and high methylation level of CG and CHG in all TE types (Fig. 4b), while the CHH contexts exhibited a low methylation level and were not obviously different in most TEs, except miniature inverted repeat transposable elements (MITE) which maintained much higher methylation levels than other types. Next, we investigated the relationship between DNA methylation and TEs length. We roughly divided the TEs into six

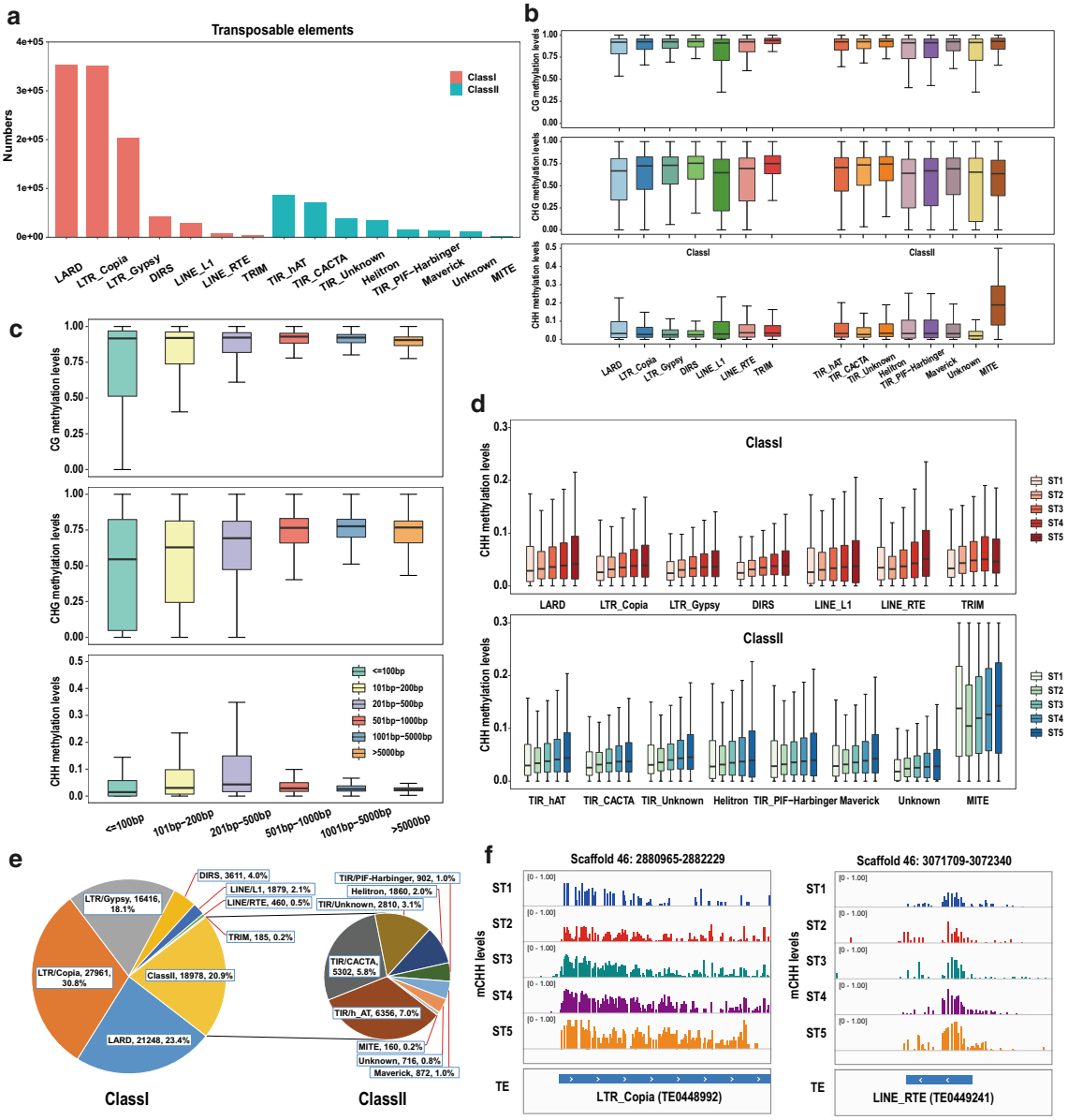

Fig. 4 Methylation profiles of different TEs in the *B. amplexicaulis* genome. **a** Numbers of different TE types. **b** Average methylation levels of different types of TEs in ST1. **c** Average methylation profiles of TEs with different length. **d** Average CHH methylation levels of Class I/Class II TEs in five different stages of shoot growth. **e** The number and percentage of TEs with increasing CHH methylation levels during the stages of shoot growth and their distribution in Class I and Class II types. **f** Two representative TEs with increasing CHH methylation levels during the shoot growth stages

groups according to their length as shown in the Fig. 4c, and found that CG methylation levels were comparable among different TEs length. On the contrary, CHG methylation levels were gradually elevated with the increase in TEs length, while CHH exhibited dynamic changes in methylation levels for different TEs length with relative high level within 200–500 bp TEs length (Figs. 4c; S5).

During bamboo internode development, CG and CHG methylation levels did not exhibit significant changes in all TE types (Fig. S6), while CHH methylation levels gradually increased in almost all TE types, except MITEs (Fig. 4d). Specifically, we totally detected 90,738 TEs whose CHH methylation level gradually increased with the developmental period (Fig. 4e). Among these TEs, there were 71,760 Class I TEs and 18,978 Class II TEs, of which LARD, LTR_Copia and LTR_Gypsy accounted for ~ 75% representing the main TE types. As shown in Fig. 4f, CHH methylation levels in two TEs (TE0448992 and TE0449241) were gradually elevated with bamboo shoot development time, while there were no obvious changes in methylation levels of CG

and CHG (Fig. S7). In sum, these results showed that DNA methylation not only had an important role in the repression of TE activity, but was also associated with development time or age, especially CHH methylation.

DNA methylation and gene expression in *B. amplexicaulis*

To investigate the relationship between DNA methylation and gene expression, we performed corresponding transcriptome analysis of the same samples using in methylome analysis (Table S4). We totally detected ~ 33,000 genes with TPM value > 0.1. Subsequently, all genes in *B. amplexicaulis* genome were divided into non-expressed genes (TPM < 0.1) and expressed genes with five groups based on their transcription levels (see Materials and methods). DNA methylation levels of all sequence contexts were then analyzed in genes body and flanking 2 kb regions. We found that the patterns were similar in different developmental stages (Fig. S8). Specifically, non-expressed genes had significantly high methylation levels of CHG and CHH in gene body regions and relatively low CG methylation in gene body regions. The genes with the highest expression levels showed the lowest CG and CHG methylation levels in the entire gene body and flanking regions (Fig. S8). We observed that genes with moderate expression levels (2nd group) had the highest CG methylation levels in gene body regions. Usually, gene body methylation was strongly associated with moderately expressed genes (Li et al. 2012). Overall, we found that CG and CHG methylation in promoter regions of genes exhibited a negative correlation with genes' expression, while CHH methylation levels seemed to have a positive correlation with genes' expression.

RNA-seq generated in this study provides us a chance to investigate the expression changes of genes related to the DNA methylation across different shoot growth stages. In total, we identified 63 methylation-related genes in *B. amplexicaulis* genome, which were listed in the Table S5. These genes were involved into the de novo DNA methylation of RdDM pathway (e.g., *BamDCL3*, *BamAGO4*, *BamDRM2* and *BamSHH1*), methylation maintenance (e.g., *BamMET1* and *BamCMT3*) and demethylation (e.g., *BamROS1* and *BamDML3*). Expression analysis revealed that all methylation-related genes were expressed in different stages of shoot development in *B. amplexicaulis* (Fig. 5; Table S5). During the rapid shoot growth stages, i.e., ST2–ST4, the demethylase genes *BamROS1* and *BamDML3* were up-regulated as compared with ST1, but the expression of methyltransferase genes *BamMET1* and *BamCMT3* were also up-regulated. The expression levels of the genes encoding demethylase exhibited much higher expression levels than genes encoding methyltransferase in ST2–ST4. Interestingly, key genes in the RdDM pathway, e.g., *BamAGO4*, *BamDRM2*, and *BamCMT2* had high expression levels throughout the whole internode developmental stages in *B. amplexicaulis*, consistent with the continuously increased CHH methylation levels. Besides, we performed the real-time quantitative polymerase chain reaction (RT-qPCR) analysis and confirmed the genes' expression in *B. amplexicaulis* internode including four DNA methyltransferase genes (*BamMET1-1*, *BamMET1-2*, *BamCMT3-1* and *BamCMT3-2*), three CHH methylation maintained-related genes (*BamCMT2*, *BamDRM2* and *BamDRM3-1*) and three demethylase genes (*BamROS1-1, BamROS1-5* and *BamDML3*) (Fig. S9).

DMRs and gene expression during the rapid shoot growth of *B. amplexicaulis*

We used the incubation stage ST1 as control to identify the DMRs for other development stages (see Materials and methods), and identified 27,668, 32,149, 34,596, 39,670 hyper-methylated DMRs and 46,738, 41,420, 39,626, 33,510 hypo-methylated DMRs in ST2, ST3, ST4 and ST5, respectively (Fig. 6a). Among these DMRs, CG-DMRs were the most abundant accounted for ~ 55%, following by CHG-DMRs (~ 25%) and CHH-DMRs (~ 20%). Meanwhile, we noted that a large number of DMRs were hypo-methylated, especially in rapid shoot growth stages (Fig. S10), which is consistent with the overall reduction of DNA methylation levels at these stages. As example of ST2 versus ST1 (ST2vST1), a key turning point from incubation period to rapid growth stages, we identified 19,376, 6910, 1382 hyper-methylated CG_DMRs, CHG_DMRs, CHH_DMRs and 21,526, 12,905, 12,307 hypo-methylated CG_DMRs, CHG_DMRs, CHH_DMRs, respectively. These DMRs were annotated to associate with 4128 hyper-methylated genes and 7359 hypo-methylated genes, and 39,961 hyper-methylated TEs and 73,923 hypo-methylated TEs (Figs. 6b; S11; Table S6). Further analysis showed that a large number of CG-DMRs occurred in the exon region (25–30%) and intergenic region (~ 45%) of genes, while CHG- and CHH-DMRs mainly located in the intergenic region (65%–70%) (Fig. 6c).

During the rapid shoot growth stages of *B. amplexicaulis*, we detected 11,058 hyper-methylated DMRs and 14,206 hypo-methylated DMRs which were shared in ST2–ST4 (Fig. 6d). As shown in Fig. 6e, these hypo-methylated DMRs shared in ST2–ST4 exhibited relatively high methylation levels at ST1, but were stable, and had lowly methylated during rapid shoot growth stages (ST2–ST4) and increased again at ST5 (Figs. 6e; S12). KEGG enrichment analysis revealed that these DMRs genes shared in ST2–ST4 stages significantly involved in plant hormone signal transduction pathways (e.g., the auxin and JA signal transduction pathways),

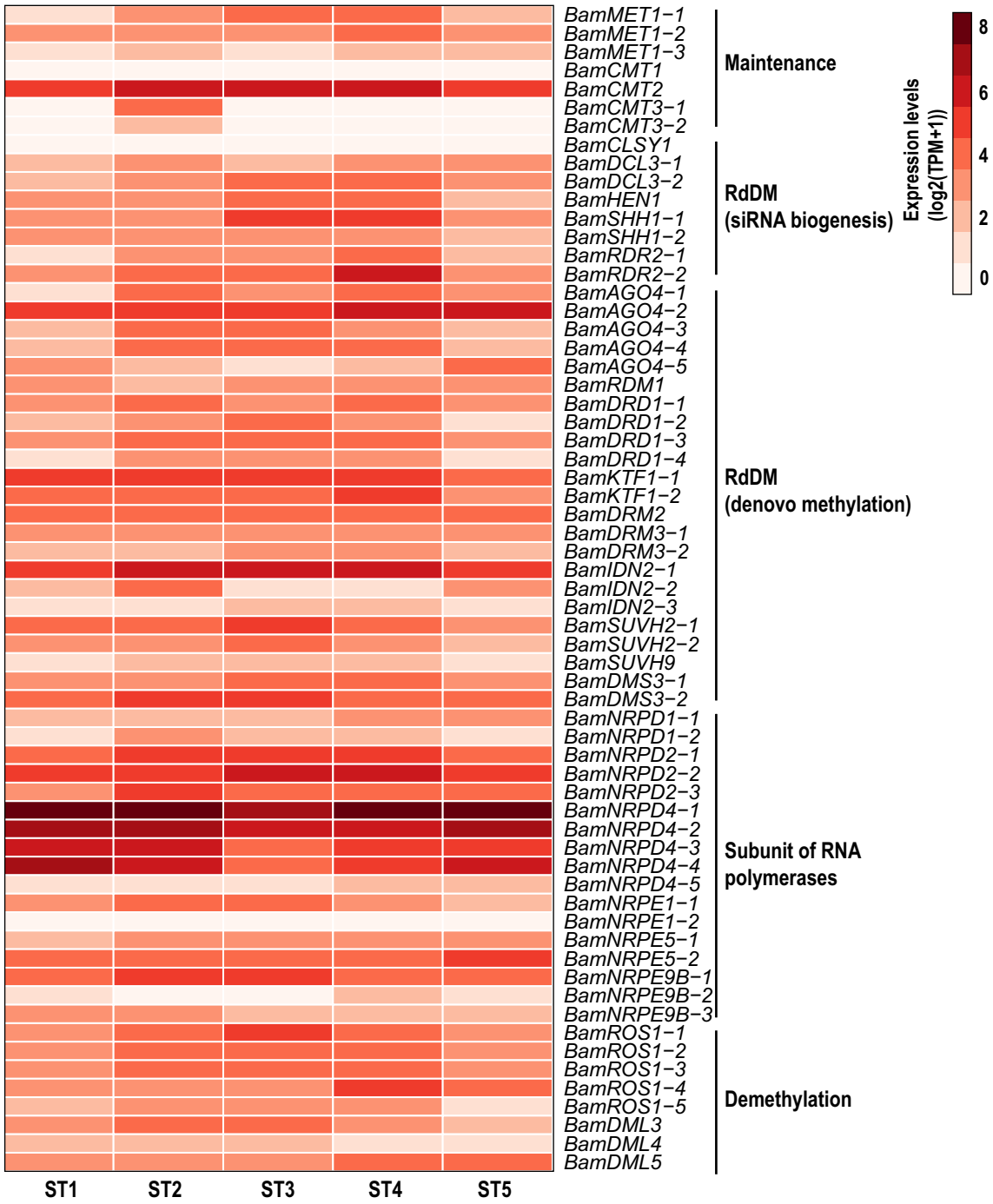

Fig. 5 Expression levels of DNA methylation-related genes in five different shoot growth stages in *B. amplexicaulis*. Expression levels were shown as $\log_2$ (TPM + 1)

spliceosome, ribosomal biosynthesis, RNA transport, and MAPK signal transduction pathways (Fig. 6f).

Accordingly, we performed the differential expression analysis based on RNA-seq data mentioned above and identified 1768, 3005, 4398, 1749 up-regulated DEGs and 2215, 4134, 6016, 2816 down-regulated DEGs identified in ST2, ST3, ST4, ST5, respectively, as compared with ST1 (Fig. 7a; Table S7). The number of DEGs was gradually increased from ST2 to ST4, and sharply reduced at ST5, suggesting the markedly transcriptional reprogramming of global gene expression patterns during shoot growth and development. Venn diagrams showed that there were 1722 DEGs overlapping in the ST2–ST4 (Fig. 7b) and the DEGs were mainly involved in protein processing in endoplasmic

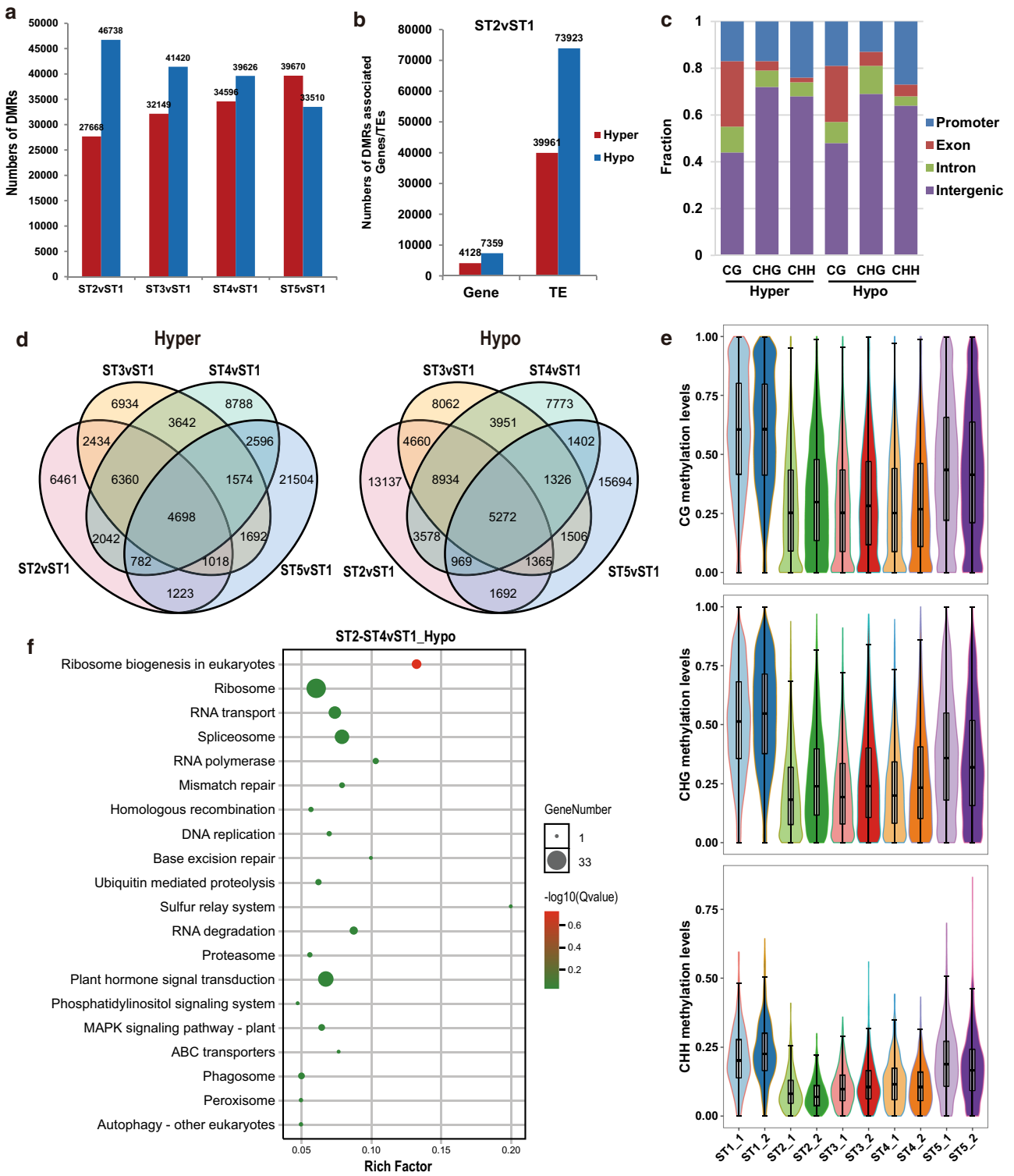

Fig. 6 Differential methylation analysis during shoot growth stages in *B. amplexicaulis*. **a** The number of DMRs in ST2–ST5 as compared with ST1. **b** Numbers of DMRs associated genes or TEs in ST2 as compared with ST1 (ST2 vs ST1). **c** The distribution of hyper and hypo DMRs in the *B. amplexicaulis* genome. **d** Overlap of hyper and hypo DMRs. **e** The methylation levels of hypo DMRs shared in ST2–ST4 across five growth stages. **f** KEGG pathway enrichment for DMRs associated genes shared in ST2–ST4. The size of the circle represents gene numbers, and the color represents the $-\log_{10} q$ value

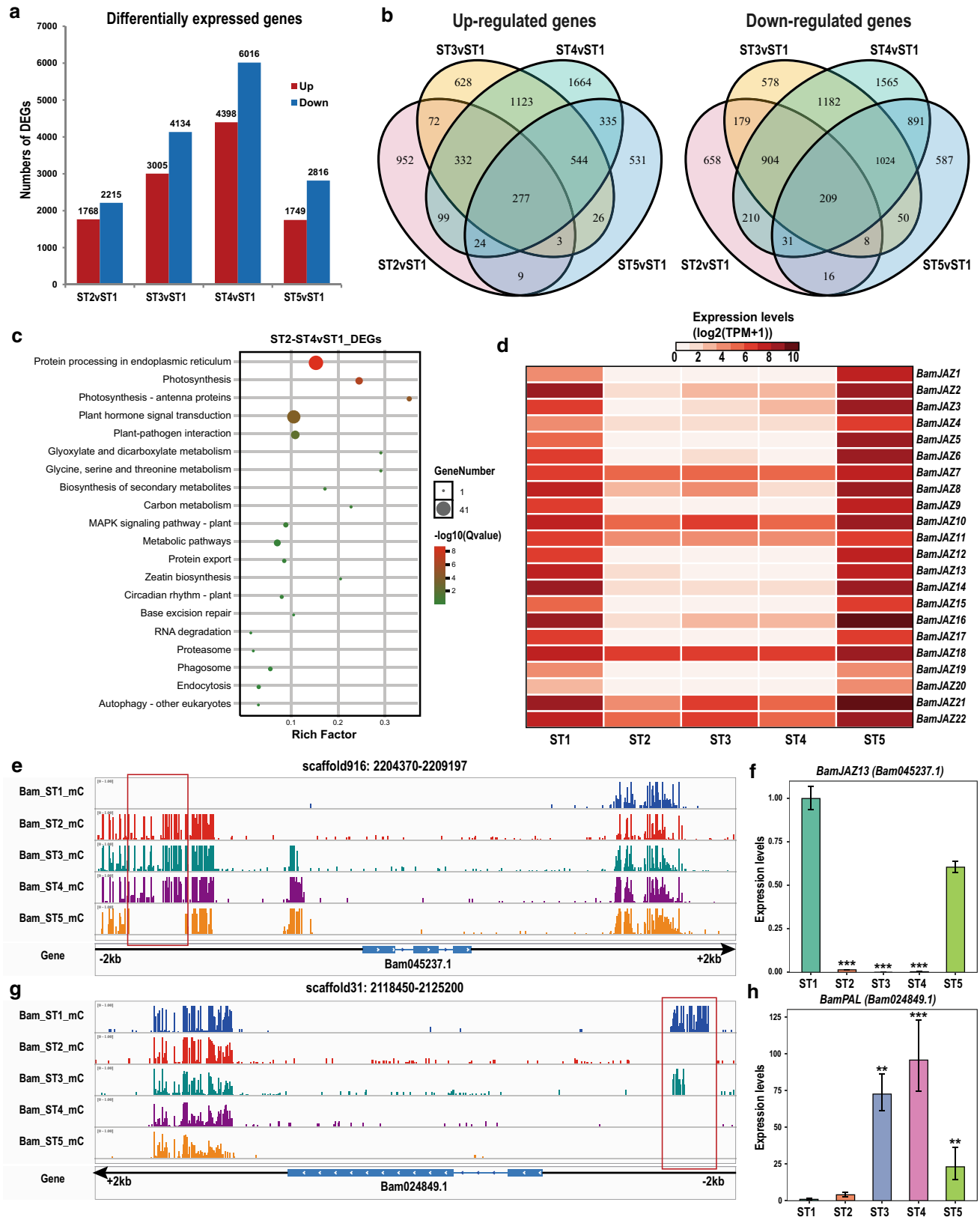
a
Differentially expressed genes
Numbers of DEGs
Up
Down
ST2vST1
ST3vST1
ST4vST1
ST5vST1
b
Up-regulated genes
Down-regulated genes
ST3vST1
ST4vST1
ST2vST1
ST5vST1
c
ST2-ST4vST1_DEGs
Protein processing in endoplasmic reticulum
Photosynthesis
Photosynthesis - antenna proteins
Plant hormone signal transduction
Plant-pathogen interaction
Glyoxylate and dicarboxylate metabolism
Glycine, serine and threonine metabolism
Biosynthesis of secondary metabolites
Carbon metabolism
MAPK signaling pathway - plant
Metabolic pathways
Protein export
Zeatin biosynthesis
Circadian rhythm - plant
Base excision repair
RNA degradation
Proteasome
Phagosome
Endocytosis
Autophagy - other eukaryotes
Rich Factor
GeneNumber
-log10(Qvalue)
d
Expression levels
(log2(TPM+1))
BamJAZ1
BamJAZ2
BamJAZ3
BamJAZ4
BamJAZ5
BamJAZ6
BamJAZ7
BamJAZ8
BamJAZ9
BamJAZ10
BamJAZ11
BamJAZ12
BamJAZ13
BamJAZ14
BamJAZ15
BamJAZ16
BamJAZ17
BamJAZ18
BamJAZ19
BamJAZ20
BamJAZ21
BamJAZ22
ST1
ST2
ST3
ST4
ST5
e
scaffold916: 2204370-2209197
Bam_ST1_mC
Bam_ST2_mC
Bam_ST3_mC
Bam_ST4_mC
Bam_ST5_mC
Gene
-2kb
Bam045237.1
+2kb
f
BamJAZ13 (Bam045237.1)
Expression levels
g
scaffold31: 2118450-2125200
Bam_ST1_mC
Bam_ST2_mC
Bam_ST3_mC
Bam_ST4_mC
Bam_ST5_mC
Gene
+2kb
Bam024849.1
-2kb
h
BamPAL (Bam024849.1)
Expression levels

◂**Fig. 7** Differentially expressed genes and DMRs during stem growth and development in *B. amplexicaulis*. **a** The numbers of DEGs in ST2–ST5 relative to ST1. **b** Overlap of the up- or down-regulated DEGs. **c** KEGG pathway enrichment for DEGs shared in ST2–ST4. The size of the circle represents gene numbers and the color represents the -$\log_{10}$ *q* value. **d** The expression profile of the *BamJAZ* genes during the shoot growth period. **e** The changes of DNA methylation in the promoter region of *BamJAZ13* during stem growth and development. **f** Relative expression levels of *BamJAZ13* at five developmental stages of the internode. **g** The changes of DNA methylation in the promoter region of *BamPAL* during stem growth and development. **h** Relative expression levels of *BamPAL* at five developmental stages of the internode. The gene *BamUBC* (*Bam040291*) encoding an ubiquitin-conjugating enzyme E2 was used as an endogenous control. Using T test for statistical analysis with ST1 as the control and significant differences calculated from the three biological replicates were indicated by * (*P* value < 0.05), ** (*P* value < 0.01) and *** (*P* value < 0.001). Error bars represented ± standard error of the mean (SE)

reticulum and photosynthesis, JA and auxin signal transduction pathways (Fig. 7c) by KEGG enrichment analysis, consistent with the result from the enrichment analysis of DMR-genes. In particular, we found that the vast majority of jasmonate ZIM-domain (JAZ) in the JA signal transduction pathway had the substantially high expression level in ST1 and ST5, but was significantly down-regulated during rapid shoot growth stages from ST2–ST4 (Fig. 7d; Table S8). JA controls a multitude of transcriptional programs affecting plant growth, development and defense by regulating gene expression and integrating with other signaling pathways (Wasternack and Hause 2013). Previous studies have revealed that JAZ is an important negative regulator in plant growth and development (Wasternack and Hause 2013; Major et al. 2017). The present result showed that JA signal transduction may have a vital role in regulating rapid shoot growth in *B. amplexicaulis*.

Specially, a gene *Bam045237* encoding JAZ13 had a high expression level during the incubation (ST1) and plateau stages (ST5), but almost no expression during the rapid shoot growth stages (ST2–ST4), which was further supported by the result from RT-qPCR analysis (Figs. 7f; S13). We detected hyper-methylated DMRs within the promoter region of the *BamJAZ13* gene in ST2–ST4, but did not found the DNA methylation at the same region in ST1 and ST2 (Figs. 7e; S14). An additional gene *Bam024849* encoding phenylalanine ammonia-lyase (PAL), a key gene involved in lignin synthesis (Barros et al. 2015), exhibited relatively high expression levels in ST2–ST5 relative to ST1. Correspondingly, we found the lack of DNA methylation in the promoter region of this gene in ST2, ST4 and ST5 and reduced methylation levels in ST3 as compared with ST1 (Figs. 7g, h; S14).

In short, these results showed that the changes of DNA methylation played a potential role in the rapid stem growth stages in *B. amplexicaulis* by activating rapid growth-induced gene expression and inhibiting rapid growth-repressed gene expression, especially the expression of genes involved in JA signal transduction.

Discussion

Understanding the rapid stem growth mechanism of woody bamboos is important to the sustainable utilization of the non-timber renewable forest resources and important progress has been made in recent years (Cui et al. 2012; Peng et al. 2013b; Tao et al. 2020; Wang et al. 2021). However, previous studies mainly focused on the cell microstructure, hormones, metabolome, transcriptome, proteome and microRNAs. The epigenetic mechanism underlying the rapid stem growth remains unclear. In addition, the rapid stem growth of woody bamboos is largely depended on the elongation of each internode (Li and Guo 2014), usually following a growth law of "slow–fast–slow" as observed in this study. However, the majority of previous studies on the rapid stem growth of woody bamboos analyzed the upper, middle or lower parts of the stems (Peng et al. 2013b) without the consideration of the heterogeneous growth stages of different internodes. In this study, we conducted DNA methylation and transcriptome analyses on a representative internode for precise characterization of the rapid stem growth of *B. amplexicaulis*, a paleotropical woody bamboo.

We detected ~ 69% CG, ~ 44% CHG and ~ 3% CHH methylation levels in the *B. amplexicaulis* genome, which is significantly lower than the overall average methylation levels in moso bamboo, *Phyllostachys edulis* with ~ 80% CG, ~ 63% CHG and ~ 3.2% CHH methylation levels (Zhang et al. 2021). One potential reason is due to the difference in genome size (850 Mb for *B. amplexicaulis* vs 2.05 Gb for moso bamboo) and TE content (54% for *B. amplexicaulis* vs 59% for moso bamboo) in two bamboo species, as previously reported in other plants (Ausin et al. 2016; Niederhuth et al. 2016). Although the DNA methylation patterns and levels varied greatly among bamboo species, the CG and CHG methylation were usually maintained at a high level especially in TE regions to guarantee the genome stability (Zhang et al. 2021). During internode growth and development, the CG and CHG methylation levels were substantially reduced in the rapid growth stages ST2–ST4, compared with the incubation stage (ST1) and plateau stage (ST5), as shown in Fig. 2b. Combined with transcriptome analysis, we found that genes encoding DNA demethylases, such as *BamROS1* and *BamDML3*, were significantly up-regulated during rapid shoot growth period (ST2–ST4) relative to ST1, which may be contributed to the reduction in DNA methylation levels to some extent, especially CG and CHG. Usually, promoter methylation of genes represses their expression and gene body methylation is positively correlated with gene

expression (Li et al. 2012). Consistent with this observation, our results reveal a negative correlation between promoter methylation of CG and CHG and gene expression, and gene body methylation of CG is associated with moderately expressed genes (see Fig. S8).

Importantly, we identified a large number of DMRs and DMR-genes shared in ST2–ST4 as compared with ST1. These shared DMR genes were mainly involved in the cell division and proliferation, auxin and JA signal transduction pathways and spliceosome. Upon transcriptome analysis, we found that DEGs shared in ST2–ST4 were also enriched in similar regulatory pathways, such as auxin and JA signal transduction. In addition, a previous study in moso bamboo demonstrated that endogenous plant hormones, such as IAA, GA3, zeatin and abscisic acid, exhibited dynamic changes during the stem growth period (Cui et al. 2012). In the present study, we found that most of JAZ-like genes in the JA signaling pathway were substantially down-regulated in the rapid shoot growth period (ST2–ST4, see Fig. 7d) and strongly associated with the heavy methylation in their promoter regions. However, the expression of JAZ-like genes exhibited high level in the incubation stage (ST1) and the plateau stage (ST5) with a lack of methylation in their promoter regions. Accumulating evidence has revealed that JAZ is an important negative regulator in plant growth and development. Studies in cotton showed that JAZ protein (GhJAZ2) inhibited fuzz fiber and lint initiation through interacting with other transcription factors to regulate the JA signaling pathway (Hu et al. 2016). JA could promote the degradation of JAZ proteins by the ubiquitination pathway and JA functions in fiber initiation and elongation (Hao et al. 2012; Major et al. 2017). Besides, we identified a hypo-methylated DMR-gene encoding PAL, a key gene for lignin synthesis; it exhibited a significantly high expression level in ST2–ST5 and a substantially low methylation levels in its promoter region at these stages. Studies have shown that rapidly elongating cells in the middle and late stages of bamboo rapid growth need to be lignified to ensure sufficient support (Chen et al. 2010; Hsieh et al. 2011; Peng et al. 2013b). In addition, we also detected a large number of hypo-methylated DMRs located in intergenic regions, and whether they have a role in the control of gene expression in a distant-acting regulatory manner remains unclear. Overall, our results revealed that DNA methylation reprogramming might have contributed to the rapid shoot growth of woody bamboos by modulating gene expression. The large number of DMRs and DEGs identified in this study provided an invaluable source for understanding the rapid shoot growth in woody bamboos.

Interestingly, we observed that the CHH methylation levels gradually accumulated in TEs and gene body regions in a time-/development-dependent manner in *B. amplexicaulis*. RNA-Seq and qRT-PCR analyses revealed that genes involved in the RdDM pathway and independent RdDM pathway exhibited high expression levels throughout the whole internode development stages in *B. amplexicaulis*, suggesting that the accumulation of CHH methylation might be related to the activity of these genes. A recent study in moso bamboo also reported a gradual increase in CHH methylation levels from the vegetative phase to the flowering phase, which is associated with the abundance of 24-nt siRNA and DRM2 expression (Zhang et al. 2021). The accumulation of CHH methylation in moso bamboo was from 5% (3-week-old seedlings) to 8% (flowering stage) in TE regions with aging. Compared with moso bamboo, *B. amplexicaulis* accumulated more CHH methylation in a shorter development time, as the CHH methylation level in TE regions increased from 4% (ST1) to 6% (ST5). These results clearly showed that CHH methylation could potentially be used as a signature of development time and aging in woody bamboos. Using DNA methylation to predict aging has been extensively reported in mammals (Levine et al. 2018; Lu et al. 2019; Wu et al. 2019). Recently, some patterns have been observed in the growth and development of plants. For example, studies revealed a globally increasing DNA methylation levels in sweet orange fruit ripening (Huang et al. 2019). This increase mainly occurred in the CHH context and was closely related to the decreased expression of DNA glycosylase genes. However, the opposite was observed in tomato fruit ripening. Active DNA demethylation mediated by *SlDML2* was central for the control of ripening in tomato and this decrease occurred in all three contexts (Lang et al. 2017). In addition, an overall loss of DNA methylation due to down-regulation of RdDM was also observed during strawberry fruit ripening (Cheng et al. 2018). These results suggest different epigenetic mechanisms during plant growth and development. Therefore, it is still unknown whether this epigenetic feature of accumulation of the CHH methylation is conserved in other plants, which is worth further inquiry.

Conclusion

Collectively, we present the DNA methylation profiles during rapid shoot growth in *B. amplexicaulis*. DNA methylation has a critical role in the regulation of the shoot growth and development, by modulating the expression of DMR genes. In particular, we discovered that a *JAZ* gene that negatively regulates the JA signaling pathway, and a key enzyme gene *PAL* for lignin synthesis were strongly associated with DNA methylation reconfiguration in their promoter regions. Although we identified a large number of DMRs, mostly located in intergenic regions, their regulatory roles need to be further determined. We discovered that CHH methylation gradually accumulated during shoot growth and development, providing new insight into understanding the relationship between DNA methylation and the development time or age of woody bamboos, as well as of other perennial plants.

Author contribution statement D-ZL and Z-HG designed and supervised the study; L-ZN collected the samples; L-ZN prepared the bisulfite and RNA sequencing; L-ZN performed methylome and transcriptome analyses; L-ZN conducted the RT-qPCR experiment; L-ZN, WX and P-FM wrote the manuscript and revised the manuscript. All authors have read and agreed the final version of the manuscript.

Supplementary Information The online version contains supplementary material available at https://doi.org/10.1007/s00425-022-03962-8.

Acknowledgements This work was supported by the Chinese Academy of Sciences' Strategic Priority Research Program (grant no. 31000000 to D.-Z.L.), and the Science and Technology Leading Talent Project of Yunnan, China (2017HA014 to D.-Z.L.), and the CAS' Youth Innovation Promotion Association (No. Y201972 to P.-F.M), and the National Natural Science Foundation of China (Project No. 31970355 to P.-F.Ma). We thank the iFlora High Performance Computing Center of Germplasm Bank of Wild Species (GBOWS) and Molecular Biology Experimental Platform of the GBOWS at Kunming Institute of Botany, Chinese Academy of Sciences for computational and experimental support.

Data availability statement Sequence data from this article can be found in the Genome Sequence Archive (SAR) repository of the National Genomics Data Center (NGDC), Beijing, China, under the accession number PRJCA010794.

Declarations

Conflict of interest The authors declare no conflict of interest.

References

Akalin A, Kormaksson M, Li S, Garrett-Bakelman FE, Figueroa ME, Melnick A, Mason CE (2012) methylKit: a comprehensive R package for the analysis of genome-wide DNA methylation profiles. Genome Biol 13:R87. https://doi.org/10.1186/gb-2012-13-10-R87

Ausin I, Feng S, Yu C, Liu W, Kuo HY, Jacobsen EL, Zhai J, Gallego-Bartolome J, Wang L, Egertsdotter U, Street NR, Jacobsen SE, Wang H (2016) DNA methylome of the 20-gigabase Norway spruce genome. Proc Natl Acad Sci USA 113:E8106–E8113. https://doi.org/10.1073/pnas.1618019113

Bailey TL, Williams N, Misleh C, Li WW (2006) MEME: discovering and analyzing DNA and protein sequence motifs. Nucleic Acids Res 34:W369-373. https://doi.org/10.1093/nar/gkl198

Barros J, Serk H, Granlund I, Pesquet E (2015) The cell biology of lignification in higher plants. Ann Bot 115:1053–1074. https://doi.org/10.1093/aob/mcv046

Bolger AM, Lohse M, Usadel B (2014) Trimmomatic: a flexible trimmer for Illumina sequence data. Bioinformatics 30:2114–2120. https://doi.org/10.1093/bioinformatics/btu170

Cao XF, Jacobsen SE (2002) Role of the *Arabidopsis DRM* methyltransferases in de novo DNA methylation and gene silencing. Curr Biol 12:1138–1144. https://doi.org/10.1016/s0960-9822(02)00925-9

Cedar H, Bergman Y (2012) Programming of DNA methylation patterns. Annu Rev Biochem 81:97–117. https://doi.org/10.1146/annurev-biochem-052610-091920

Chen CY, Hsieh MH, Yang CC, Lin CS, Wang AY (2010) Analysis of the cellulose synthase genes associated with primary cell wall synthesis in *Bambusa oldhamii*. Phytochemistry 71:1270–1279. https://doi.org/10.1016/j.phytochem.2010.05.011

Cheng J, Niu Q, Zhang B, Chen K, Yang R, Zhu JK, Zhang Y, Lang Z (2018) Downregulation of RdDM during strawberry fruit ripening. Genome Biol 19:212. https://doi.org/10.1186/s13059-018-1587-x

Chiu WB, Lin CH, Chang CJ, Hsieh MH, Wang AY (2006) Molecular characterization and expression of four cDNAs encoding sucrose synthase from green bamboo *Bambusa oldhamii*. New Phytol 170:53–63. https://doi.org/10.1111/j.1469-8137.2005.01638.x

Choi YH, Gehring M, Johnson L, Hannon M, Harada JJ, Goldberg RB, Jacobsen SE, Fischer RL (2002) DEMETER, a DNA glycosylase domain protein, is required for endosperm gene imprinting and seed viability in *Arabidopsis*. Cell 110:33–42. https://doi.org/10.1016/s0092-8674(02)00807-3

Cui K, He C-Y, Zhang J-G, Duan A-G, Zeng Y-F (2012) Temporal and spatial profiling of internode elongation-associated protein expression in rapidly growing culms of bamboo. J Proteome Res 11:2492–2507. https://doi.org/10.1021/pr2011878

Du J, Zhong X, Bernatavichute YV, Stroud H, Feng S, Caro E, Vashisht AA, Terragni J, Chin HG, Tu A, Hetzel J, Wohlschlegel JA, Pradhan S, Patel DJ, Jacobsen SE (2012) Dual binding of chromomethylase domains to H3K9me2-containing nucleosomes directs DNA methylation in plants. Cell 151:167–180. https://doi.org/10.1016/j.cell.2012.07.034

Ebbs ML, Bartee L, Bender J (2005) H3 lysine 9 methylation is maintained on a transcribed inverted repeat by combined action of SUVH6 and SUVH4 methyltransferases. Mol Cell Biol 25:10507–10515. https://doi.org/10.1128/MCB.25.23.10507-10515.2005

Feng S, Jacobsen SE, Reik W (2010) Epigenetic reprogramming in plant and animal development. Science 330:622–627. https://doi.org/10.1126/science.1190614

Finnegan EJ, Dennis ES (1993) Isolation and identification by sequence homology of a putative cytosine methyltransferase from *Arabidopsis thaliana*. Nucleic Acids Res 21:2383–2388. https://doi.org/10.1093/nar/21.10.2383

Finnegan EJ, Peacock WJ, Dennis ES (1996) Reduced DNA methylation in *Arabidopsis thaliana* results in abnormal plant development. Proc Natl Acad Sci USA 93:8449–8454. https://doi.org/10.1073/pnas.93.16.8449

Gao Z, Yang X, Peng Z, Li X, Mu S, Ma Y (2010) Molecular characterization-and subceilular localization of *BoSUT2* from *Bambusa oldhamii*. Sci Silvae Sin 46:45–50. https://doi.org/10.11707/j.1001-7488.20100208

Garcia-Aguilar M, Michaud C, Leblanc O, Grimanelli D (2010) Inactivation of a DNA methylation pathway in maize reproductive organs results in apomixis-like phenotypes. Plant Cell 22:3249–3267. https://doi.org/10.1105/tpc.109.072181

Ginestet C (2011) ggplot2: elegant graphics for data analysis. J R Stat Soc Ser A (stat Soc) 174:245–245. https://doi.org/10.1111/j.1467-985X.2010.00676_9.x

Gong ZH, Morales-Ruiz T, Ariza RR, Roldan-Arjona T, David L, Zhu JK (2002) *ROS1*, a repressor of transcriptional gene silencing in *Arabidopsis*, encodes a DNA glycosylase/lyase. Cell 111:803–814. https://doi.org/10.1016/s0092-8674(02)01133-9

Gouil Q, Baulcombe DC (2016) DNA methylation signatures of the plant chromomethyltransferases. PLoS Genet 12:e1006526. https://doi.org/10.1371/journal.pgen.1006526

Guo ZH, Ma PF, Yang GQ, Hu JY, Liu YL, Xia EH, Zhong MC, Zhao L, Sun GL, Xu YX, Zhao YJ, Zhang YC, Zhang YX, Zhang XM, Zhou MY, Guo Y, Guo C, Liu JX, Ye XY, Chen YM, Yang Y, Han B, Lin CS, Lu Y, Li DZ (2019) Genome sequences provide insights into the reticulate origin and unique

traits of woody bamboos. Mol Plant 12:1353–1365. https://doi.org/10.1016/j.molp.2019.05.009
Hao J, Tu L, Hu H, Tan J, Deng F, Tang W, Nie Y, Zhang X (2012) GbTCP, a cotton TCP transcription factor, confers fibre elongation and root hair development by a complex regulating system. J Exp Bot 63:6267–6281. https://doi.org/10.1093/jxb/ers278
Hsieh L-S, Yeh C-S, Pan H-C, Cheng C-Y, Yang C-C, Lee P-D (2010a) Cloning and expression of a phenylalanine ammonia-lyase gene (*BoPAL2*) from *Bambusa oldhamii* in *Escherichia coli* and *Pichia pastoris*. Protein Express Purif 71:224–230. https://doi.org/10.1016/j.pep.2010.01.009
Hsieh LS, Ma GJ, Yang CC, Lee PD (2010b) Cloning, expression, site-directed mutagenesis and immunolocalization of phenylalanine ammonia-lyase in *Bambusa oldhamii*. Phytochemistry 71:1999–2009. https://doi.org/10.1016/j.phytochem.2010.09.019
Hsieh LS, Hsieh YL, Yeh CS, Cheng CY, Yang CC, Lee PD (2011) Molecular characterization of a phenylalanine ammonia-lyase gene (*BoPAL1*) from *Bambusa oldhamii*. Mol Biol Rep 38:283–290. https://doi.org/10.1007/s11033-010-0106-2
Hu H, He X, Tu L, Zhu L, Zhu S, Ge Z, Zhang X (2016) GhJAZ2 negatively regulates cotton fiber initiation by interacting with the R2R3-MYB transcription factor GhMYB25-like. Plant J 88:921–935. https://doi.org/10.1111/tpj.13273
Huang X, Zhang S, Li K, Thimmapuram J, Xie S (2018) ViewBS: a powerful toolkit for visualization of high-throughput bisulfite sequencing data. Bioinformatics 34:708–709. https://doi.org/10.1093/bioinformatics/btx633
Huang H, Liu R, Niu Q, Tang K, Zhang B, Zhang H, Chen K, Zhu JK, Lang Z (2019) Global increase in DNA methylation during orange fruit development and ripening. Proc Natl Acad Sci USA 116:1430–1436. https://doi.org/10.1073/pnas.1815441116
Jackson JP, Johnson L, Jasencakova Z, Zhang X, PerezBurgos L, Singh PB, Cheng X, Schubert I, Jenuwein T, Jacobsen SE (2004) Dimethylation of histone H3 lysine 9 is a critical mark for DNA methylation and gene silencing in *Arabidopsis thaliana*. Chromosoma 112:308–315. https://doi.org/10.1007/s00412-004-0275-7
Janzen DH (1976) Why bamboos wait so long to flower. Annu Rev Ecol Syst 7:347–391. https://doi.org/10.1146/annurev.es.07.110176.002023
Jin GH, Ma PF, Wu XP, Gu LF, Long M, Zhang CJ, Li DZ (2021) New genes interacted with recent whole genome duplicates in the fast stem growth of bamboos. Mol Biol Evol 38:5752–5768. https://doi.org/10.1093/molbev/msab288
Kankel MW, Ramsey DE, Stokes TL, Flowers SK, Haag JR, Jeddeloh JA, Riddle NC, Verbsky ML, Richards EJ (2003) *Arabidopsis MET1* cytosine methyltransferase mutants. Genetics 163:1109–1122. https://doi.org/10.1093/genetics/163.3.1109
Kim D, Paggi JM, Park C, Bennett C, Salzberg SL (2019) Graph-based genome alignment and genotyping with HISAT2 and HISAT-genotype. Nat Biotechnol 37:907–915. https://doi.org/10.1038/s41587-019-0201-4
Krueger F, Andrews SR (2011) Bismark: a flexible aligner and methylation caller for Bisulfite-Seq applications. Bioinformatics 27:1571–1572. https://doi.org/10.1093/bioinformatics/btr167
Lang Z, Wang Y, Tang K, Tang D, Datsenka T, Cheng J, Zhang Y, Handa AK, Zhu JK (2017) Critical roles of DNA demethylation in the activation of ripening-induced genes and inhibition of ripening-repressed genes in tomato fruit. Proc Natl Acad Sci USA 114:E4511–E4519. https://doi.org/10.1073/pnas.1705233114
Langmead B, Salzberg SL (2012) Fast gapped-read alignment with Bowtie 2. Nat Methods 9:357–359. https://doi.org/10.1038/nmeth.1923
Law JA, Jacobsen SE (2010) Establishing, maintaining and modifying DNA methylation patterns in plants and animals. Nat Rev Genet 11:204–220. https://doi.org/10.1038/nrg2719
Letunic I, Copley RR, Schmidt S, Ciccarelli FD, Doerks T, Schultz J, Ponting CP, Bork P (2004) SMART 4.0: towards genomic data integration. Nucleic Acids Res 32::D142-D144. https://doi.org/10.1093/nar/gkh088
Levine ME, Lu AT, Quach A, Chen BH, Assimes TL, Bandinelli S, Hou L, Baccarelli AA, Stewart JD, Li Y, Whitsel EA, Wilson JG, Reiner AP, Aviv A, Lohman K, Liu Y, Ferrucci L, Horvath S (2018) An epigenetic biomarker of aging for lifespan and healthspan. Aging-Us 10:573–591. https://doi.org/10.18632/aging.101414
Li X, Guo Z-H (2014) A pilot study on internode elongation in a paleotropical bamboo, *Dendrocalamus latiflorus* (Poaceae: Bambusoideae). Plant Divers Resour 36:22–28. https://doi.org/10.7677/ynzwyj201413075
Li DZ, Wang ZP, Zhu ZD, Xia NH, Jia LZ, Guo ZH, Yang GY, Stapleton C (2006) Bambuseae (Poaceae). Flora of China, vol 22. Science Press and Missouri Botanical Garden Press, Beijing, pp 7–180
Li X, Zhu J, Hu F, Ge S, Ye M, Xiang H, Zhang G, Zheng X, Zhang H, Zhang S, Li Q, Luo R, Yu C, Yu J, Sun J, Zou X, Cao X, Xie X, Wang J, Wang W (2012) Single-base resolution maps of cultivated and wild rice methylomes and regulatory roles of DNA methylation in plant gene expression. BMC Genom 13:300. https://doi.org/10.1186/1471-2164-13-300
Li Q, Eichten SR, Hermanson PJ, Zaunbrecher VM, Song J, Wendt J, Rosenbaum H, Madzima TF, Sloan AE, Huang J, Burgess DL, Richmond TA, McGinnis KM, Meeley RB, Danilevskaya ON, Vaughn MW, Kaeppler SM, Jeddeloh JA, Springer NM (2014) Genetic perturbation of the maize methylome. Plant Cell 26:4602–4616. https://doi.org/10.1105/tpc.114.133140
Lin JX, He XQ, Hu YX, Kuang TY, Ceulemans R (2002) Lignification and lignin heterogeneity for various age classes of bamboo (*Phyllostachys pubescens*) stems. Physiol Plant 114:296–302. https://doi.org/10.1034/j.1399-3054.2002.1140216.x
Lindroth AM, Cao X, Jackson JP, Zilberman D, McCallum CM, Henikoff S, Jacobsen SE (2001) Requirement of *CHROMOMETHYLASE3* for maintenance of CpXpG methylation. Science 292:2077–2080. https://doi.org/10.1126/science.1059745
Liu M, Qiao G, Jiang J, Yang H, Xie L, Xie J, Zhuo R (2012) Transcriptome sequencing and *de novo* analysis for Ma bamboo (*Dendrocalamus latiflorus* Munro) using the illumina platform. PLoS ONE 7:e46766. https://doi.org/10.1371/journal.pone.0046766
Lu AT, Quach A, Wilson JG, Reiner AP, Aviv A, Raj K, Hou L, Baccarelli AA, Li Y, Stewart JD, Whitsel EA, Assimes TL, Ferrucci L, Horvath S (2019) DNA methylation GrimAge strongly predicts lifespan and healthspan. Aging-Us 11:303–327. https://doi.org/10.18632/aging.101684
Major IT, Yoshida Y, Campos ML, Kapali G, Xin XF, Sugimoto K, de Oliveira FD, He SY, Howe GA (2017) Regulation of growth-defense balance by the JASMONATE ZIM-DOMAIN (JAZ)-MYC transcriptional module. New Phytol 215:1533–1547. https://doi.org/10.1111/nph.14638
Matzke MA, Mosher RA (2014) RNA-directed DNA methylation: an epigenetic pathway of increasing complexity. Nat Rev Genet 15:394–408. https://doi.org/10.1038/nrg3683
Mistry J, Chuguransky S, Williams L, Qureshi M, Salazar GA, Sonnhammer ELL, Tosatto SCE, Paladin L, Raj S, Richardson LJ, Finn RD, Bateman A (2021) Pfam: The protein families database in 2021. Nucleic Acids Res 49:D412–D419. https://doi.org/10.1093/nar/gkaa913
Moritoh S, Eun CH, Ono A, Asao H, Okano Y, Yamaguchi K, Shimatani Z, Koizumi A, Terada R (2012) Targeted disruption of an orthologue of *DOMAINS REARRANGED METHYLASE 2*,

OsDRM2, impairs the growth of rice plants by abnormal DNA methylation. Plant J 71:85–98. https://doi.org/10.1111/j.1365-313X.2012.04974.x

Murphy RJ, Alvin KL (1992) Variation in fiber wall structure in bamboo. Iawa Bull 13:403–410. https://doi.org/10.1163/22941932-90001296

Nakano Y, Steward N, Sekine M, Kusano T, Sano H (2000) A tobacco *NtMET1* cDNA encoding a DNA methyltransferase: molecular characterization and abnormal phenotypes of transgenic tobacco plants. Plant Cell Physiol 41:448–457. https://doi.org/10.1093/pcp/41.4.448

Niederhuth CE, Bewick AJ, Ji L, Alabady MS, Kim KD, Li Q, Rohr NA, Rambani A, Burke JM, Udall JA, Egesi C, Schmutz J, Grimwood J, Jackson SA, Springer NM, Schmitz RJ (2016) Widespread natural variation of DNA methylation within angiosperms. Genome Biol 17:194. https://doi.org/10.1186/s13059-016-1059-0

Ortega-Galisteo AP, Morales-Ruiz T, Ariza RR, Roldan-Arjona T (2008) *Arabidopsis* DEMETER-LIKE proteins DML2 and DML3 are required for appropriate distribution of DNA methylation marks. Plant Mol Biol 67:671–681. https://doi.org/10.1007/s11103-008-9346-0

Park K, Kim MY, Vickers M, Park JS, Hyun Y, Okamoto T, Zilberman D, Fischer RL, Feng X, Choi Y, Scholten S (2016) DNA demethylation is initiated in the central cells of *Arabidopsis* and rice. Proc Natl Acad Sci USA 113:15138–15143. https://doi.org/10.1073/pnas.1619047114

Peng Z, Lu Y, Li L, Zhao Q, Feng Q, Gao Z, Lu H, Hu T, Yao N, Liu K, Li Y, Fan D, Guo Y, Li W, Lu Y, Weng Q, Zhou C, Zhang L, Huang T, Zhao Y, Zhu C, Liu X, Yang X, Wang T, Miao K, Zhuang C, Cao X, Tang W, Liu G, Liu Y, Chen J, Liu Z, Yuan L, Liu Z, Huang X, Lu T, Fei B, Ning Z, Han B, Jiang Z (2013a) The draft genome of the fast-growing non-timber forest species moso bamboo (*Phyllostachys heterocycla*). Nat Genet 45:456–461. https://doi.org/10.1038/ng.2569

Peng Z, Zhang C, Zhang Y, Hu T, Mu S, Li X, Gao J (2013b) Transcriptome sequencing and analysis of the fast growing shoots of moso bamboo (*Phyllostachys edulis*). PLoS ONE 8:e78944. https://doi.org/10.1371/journal.pone.0078944

Penterman J, Zilberman D, Huh JH, Ballinger T, Henikoff S, Fischer RL (2007) DNA demethylation in the *Arabidopsis* genome. Proc Natl Acad Sci USA 104:6752–6757. https://doi.org/10.1073/pnas.0701861104

Quinlan AR, Hall IM (2010) BEDTools: a flexible suite of utilities for comparing genomic features. Bioinformatics 26:841–842. https://doi.org/10.1093/bioinformatics/btq033

Soreng RJ, Peterson PM, Zuloaga FO, Romaschenko K, Clark LG, Teisher JK, Gillespie LJ, Barberá P, Welker CAD, Kellogg EA, Li DZ, Davidse G (2022) A worldwide phylogenetic classification of the Poaceae (Gramineae) III: an update. J Syst Evol 60:476–521. https://doi.org/10.1111/jse.12847

Stroud H, Greenberg MV, Feng S, Bernatavichute YV, Jacobsen SE (2013) Comprehensive analysis of silencing mutants reveals complex regulation of the *Arabidopsis* methylome. Cell 152:352–364. https://doi.org/10.1016/j.cell.2012.10.054

Stroud H, Do T, Du J, Zhong X, Feng S, Johnson L, Patel DJ, Jacobsen SE (2014) Non-CG methylation patterns shape the epigenetic landscape in *Arabidopsis*. Nat Struct Mol Biol 21:64–72. https://doi.org/10.1038/nsmb.2735

Tamura K, Stecher G, Peterson D, Filipski A, Kumar S (2013) MEGA6: molecular evolutionary genetics analysis version 6.0. Mol Biol Evol 30:2725–2729. https://doi.org/10.1093/molbev/mst197

Tang H, Liu W, Huang T, Jiang LY, Huang CQ, Huang WT (2015) Study on shooting and young bamboo height growth of *Phyllostachys heterocycla* in Hunan Forest Botanical Garden. J Cent South Univ for Technol 35:27–31. https://doi.org/10.14067/j.cnki.1673-923x.2015.08.006

Tao GY, Ramakrishnan M, Vinod KK, Yrjala K, Satheesh V, Cho J, Fu Y, Zhou M (2020) Multi-omics analysis of cellular pathways involved in different rapid growth stages of moso bamboo. Tree Physiol 40:1487–1508. https://doi.org/10.1093/treephys/tpaa090

Thorvaldsdottir H, Robinson JT, Mesirov JP (2013) Integrative Genomics Viewer (IGV): high-performance genomics data visualization and exploration. Briefings Bioinform 14:178–192. https://doi.org/10.1093/bib/bbs017

Varet H, Brillet-Gueguen L, Coppee JY, Dillies MA (2016) SARTools: a DESeq2- and edgeR-based R pipeline for comprehensive differential analysis of RNA-Seq data. PLoS ONE 11:e0157022. https://doi.org/10.1371/journal.pone.0157022

Wang KL, Zhang Y, Zhang HM, Lin XC, Xia R, Song L, Wu AM (2021) MicroRNAs play important roles in regulating the rapid growth of the *Phyllostachys edulis* culm internode. New Phytol 231:2215–2230. https://doi.org/10.1111/nph.17542

Wasternack C, Hause B (2013) Jasmonates: biosynthesis, perception, signal transduction and action in plant stress response, growth and development. An update to the 2007 review in *Annals of Botany*. Ann Bot 111:1021–1058. https://doi.org/10.1093/aob/mct067

Wei L, Gu L, Song X, Cui X, Lu Z, Zhou M, Wang L, Hu F, Zhai J, Meyers BC, Cao X (2014) Dicer-like 3 produces transposable element-associated 24-nt siRNAs that control agricultural traits in rice. Proc Natl Acad Sci USA 111:3877–3882. https://doi.org/10.1073/pnas.1318131111

Wu X, Chen W, Lin F, Huang Q, Zhong J, Gao H, Song Y, Liang H (2019) DNA methylation profile is a quantitative measure of biological aging in children. Aging-Us 11:10031–10051. https://doi.org/10.18632/aging.102399

Xie Z, Johansen LK, Gustafson AM, Kasschau KD, Lellis AD, Zilberman D, Jacobsen SE, Carrington JC (2004) Genetic and functional diversification of small RNA pathways in plants. PLoS Biol 2:e104. https://doi.org/10.1371/journal.pbio.0020104

Yamauchi T, Johzuka-Hisatomi Y, Terada R, Nakamura I, Iida S (2014) The *MET1b* gene encoding a maintenance DNA methyltransferase is indispensable for normal development in rice. Plant Mol Biol 85:219–232. https://doi.org/10.1007/s11103-014-0178-9

Zemach A, Kim MY, Hsieh PH, Coleman-Derr D, Eshed-Williams L, Thao K, Harmer SL, Zilberman D (2013) The *Arabidopsis* nucleosome remodeler DDM1 allows DNA methyltransferases to access H1-containing heterochromatin. Cell 153:193–205. https://doi.org/10.1016/j.cell.2013.02.033

Zhang H, Lang Z, Zhu JK (2018) Dynamics and function of DNA methylation in plants. Nat Rev Mol Cell Biol 19:489–506. https://doi.org/10.1038/s41580-018-0016-z

Zhang Z, Wang H, Wang Y, Xi F, Wang H, Kohnen MV, Gao P, Wei W, Chen K, Liu X, Gao Y, Han X, Hu K, Zhang H, Zhu Q, Zheng Y, Liu B, Ahmad A, Hsu YH, Jacobsen SE, Gu L (2021) Whole-genome characterization of chronological age-associated changes in methylome and circular RNAs in moso bamboo (*Phyllostachys edulis*) from vegetative to floral growth. Plant J 106:435–453. https://doi.org/10.1111/tpj.15174

Publisher's Note Springer Nature remains neutral with regard to jurisdictional claims in published maps and institutional affiliations.

Springer Nature or its licensor holds exclusive rights to this article under a publishing agreement with the author(s) or other rightsholder(s); author self-archiving of the accepted manuscript version of this article is solely governed by the terms of such publishing agreement and applicable law.